Study on Single-Polarized Holey Fibers with Double-Hole Unit Cores for Cross-Talk Free Polarization Splitter

IEICE TRANS. ELECTRON., VOL.E101–C, NO.8 AUGUST 2018

PAPER Special Section on Recent Advances in Simulation Techniques and Their Applications for Electronics

Study on Single-Polarized Holey Fibers with Double-Hole Unit Cores for Cross-Talk Free Polarization Splitter

Zejun ZHANG[†a)], ***Nonmember***, **Yasuhide TSUJI**[††], **Masashi EGUCHI**[†††], ***and*** **Chun-ping CHEN**[†], ***Members***

SUMMARY A single-polarization single-mode (SPSM) photonic crystal fiber (PCF) based on double-hole unit core is proposed in this paper for application to cross-talk free polarization splitter (PS). Birefringence of the PCF is obtained by adopting double-hole unit cells into the core to destroy its symmetry. With an appropriate cladding hole size, single *x*- or *y*-polarized PCF can be achieved by arranging the double-hole unit in the core along the *x*- or *y*-axis, respectively. Moreover, our proposed SPSM PCF has the potential to be applied to consist a cross-talk free PS. The simulation result by employing a vectorial finite element beam propagation method (FE-BPM) demonstrates that an arbitrary polarized incident light can be completely separated into two orthogonal single-polarized components through the PS. The structural tolerance and wavelength dependence of the PS have also been discussed in detail.

key words: *single-polarization single-mode, photonic crystal fiber, polarization splitter*

1. Introduction

With the continuous development of information society and the rapid popularization of the Internet, the demand for high-speed large-capacity optical communication system is further increased. In the past two decades, study on high-performance optical devices based on photonic crystal fibers (PCFs) [1], [2] attracts a lot of attention of researchers. PCFs or micro-structured optical fibers are special types of optical fibers where air holes are arranged in a periodic arrangement in the cladding. According to the different guidance mechanisms, PCFs are generally classified into two categories: the holey fiber (HF) [3] based on the total internal reflection mechanism and the photonic band gap fiber (PBGF) [4] based on the photonic band gap of periodic structure. In comparison to conventional optical fibers, PCF shows basic properties including high birefringence, nonlinearity, endless single-mode, *etc*.. Among them, the PCF with high birefringence [5]–[7], which can be obtained by breaking the symmetry of core or the cladding, is a key concern for coherent communication and is widely used to design a single-polarization single-mode (SPSM) fiber [3]. A SPSM PCF guides only one polarization mode and thus eliminates the mode coupling between the two orthogonally polarized fundamental modes. Compared with the conventional polarization-maintaining (PM) fibers that support two orthogonal polarization states, a SPSM PCF offers several advantages including a high extinction ratio, no polarization mode dispersion, and polarization-dependent loss issues. So far, a number of SPSM PCFs [8]–[11] with various periodic lattices have been proposed.

In the modern information society, polarization splitters (PSs), which can split an arbitrary polarized light into two orthogonal polarization states, are widely studied as one of the key element in optical communication system. So far, several PCF based PSs have been proposed [12]–[15]. For the general PSs, polarization splitting is achieved by separating one of the orthogonal polarization state (*x*- or *y*-polarized component) out of the incident beam using the different coupling lengths of the two polarized components. However, this kind of PSs suffer a long device length and the unavoidable extinction ratio. In 2014, Zhang *et al*. proposed a novel cross-talk free PS based on special SPSM PCFs whose core consists of elliptical-hole unit [14]. Although this device has a cross-talk free property and a short device length, it is suffering a low structural tolerance due to the fluctuation during manufacturing processes of the elliptical air hole. After that, Zhong *et al*. studied an L-shaped PS with square lattice SPSM PCFs which has a high structural tolerance [15]. However, the distribution of the output pattern is not a Gaussian distribution, which may cause a large splice loss with a conventional fiber. Therefore, considering the PCF fabrication technology, an SPSM PCF with only circular air holes should be discussed for application to the cross-talk free PS.

In this study, a novel hexagonal lattice single-polarization holey fiber (SPHF) with an asymmetric core is proposed. Instead of the difficult elliptical-hole cells, double-hole unit cells are introduced into the core to break the symmetry. With an appropriate cladding hole size, the singe *x*- or *y*-polarized PCF can be achieved by arranging the double-hole unit along the *x*- or *y*-axis, respectively. Additionally, in order to achieve a cross-talk free PS, the phase matched *x*-polarized SPHF (*x*SPHF) and *y*-polarized SPHF (*y*SPHF) are designed. In this research, the full-vectorial finite element method (FV-FEM) [16] and the finite element beam propagation method (FE-BPM) [17] have been used to estimate the modal effective index of each waveguide and the light propagation, respectively.

Manuscript received November 2, 2017.
Manuscript revised March 8, 2018.

[†]The authors are with Department of Electrical, Electronics and Information Eng., Kanagawa University, Yokohama-shi, 221–8686 Japan.
[††]The author is with Information and Electronic Eng., Muroran Institute of Technology, Muroran-shi, 050–8585 Japan.
[†††]The author is with Department of Opt-Electronic System Eng., Chitose Institute of Science and Technology, Chitose-shi, 066–8655 Japan.
a) E-mail: zhang-zj17@kanagawa-u.ac.jp

DOI: 10.1587/transele.E101.C.620

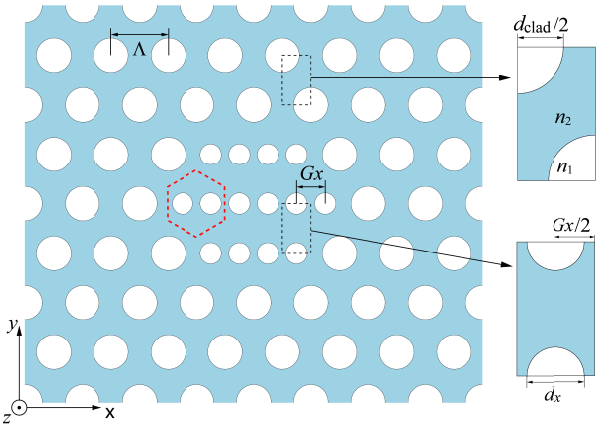

Fig. 1 Cross section of an *x*SPHF with double-hole units in the core. One unit hexagonal cell is represented by red thick dashed frame in which two circular air holes is arranged along the *x* direction.

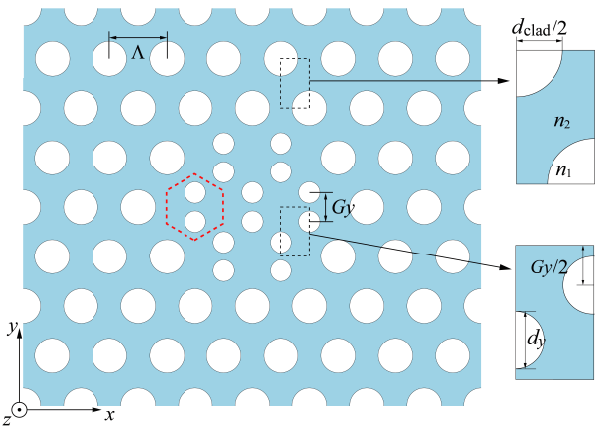

Fig. 2 Cross section of a *y*SPHF with double-hole units in the core. One unit hexagonal cell is represented by red thick dashed frame in which two circular air holes is arranged along the *y* direction.

2. Birefringence with Double-Hole Unit

In this section, the birefringence of PCF with double-hole units in the core is discussed. Since the geometry of double holes affects the core birefringence, we discuss the core birefringence variation with different hole sizes and positions by investigating the fundamental space-filling mode (FSM) of the core unit cell.

As we know, a conventional holey fiber with a hexagonal lattice of air holes around the core has an isotropic property. We consider that the core birefringence can be realized by adopting several double-hole unit cells into the core region. Figures 1 and 2 illustrate the cross sectional views of a 1-ring core *x*SPHF and *y*SPHF, respectively. For each unit cell in the core region (shown in a red hexagonal dashed frame), two circular holes are arranged along the *x*- or *y*-direction, respectively. By introducing these kinds of double-hole units to replace the elliptical-hole units, highly birefringent HF can be obtained. The light blue region indicates silica, and the white circular holes indicate air holes.

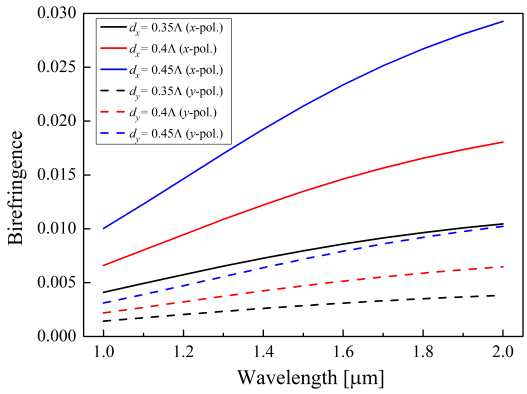

Fig. 3 Variation of the core birefringence against the normalized wavelength for each SPHF with constant core gaps $G_x = G_y = 0.5\Lambda$.

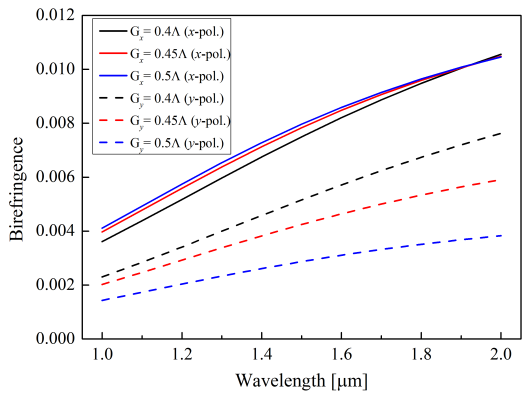

Fig. 4 Variation of the core birefringence against the normalized wavelength for each SPHF with constant core sizes $d_x = d_y = 0.35\Lambda$.

The refractive indices of the silica and air hole are set to $n_1 = 1.45$ and $n_2 = 1$, respectively. According to [18], Mägi *et al*. fabricated a tapered PCF with a minimum lattice pitch less than 300 nm using the post-processing technique and the flame brushing technique in 2004. Therefore, the PCF with the lattice pitch up to micron level can be produced under the current production technology. In this study, a lattice pitch $\Lambda = 2\ \mu$m is adopted to design the SPHF. In order to ensure SPHFs with double-hole units have the same air-filling fraction the EC-CHF in [14], the original structural parameters of these two HFs are given as follows: the diameter of holes in the double-hole unit cell for each SPHF is set to $d_x = d_y = 0.45\Lambda$, the hole gap is set to $G_x = G_y = 0.5\Lambda$. The unit cells used for FSM analysis are also illustrated in Figs. 1 and 2. The core birefringence of HF is defined as

$$\Delta n = |n_{\text{eff}}^x - n_{\text{eff}}^y| \tag{1}$$

where n_{eff}^x and n_{eff}^y are the effective indices of FSM in the core for the *x*- and *y*-polarization, respectively.

For the asymmetric core, the birefringence is sensitive to the double-hole geometry. Here, the hole size and hole gap dependence of birefringence is investigated, as shown in Figs. 3 and 4, respectively. In Fig. 3, the hole gaps G_x and G_y are maintained at 0.5Λ, the birefringence variation

of xSPHF and ySPHF are respectively represented by the solid and dashed curves with $d_x = d_y = 0.35\Lambda$, 0.4Λ, and 0.45Λ. The birefringence increases by increasing the normalized wavelength, and the large hole size leads to a large birefringence for both SPHFs. Moreover, the xSPHF has a lager birefringence than that of the ySPHF with the same hole size due to their different hole arrangement. Considering fabrication process, the hole diameter should be less than the hole gap in an unit cell, and the manufacturing difficulty will increase if the two air holes are too close to each other, we fix the core hole size to 0.35Λ. Figure 4 illustrates the variation of birefringence with different hole gaps where the hole sizes are set to $d_x = d_y = 0.35\Lambda$. For the xSPHF core region, since each row of air holes is arranged adjacent to each other, the birefringence reaches the maximum with $G_x = 0.5\Lambda$. On the contrary, with a constant circular hole size, the small hole gap leads to a high birefringence for the ySPHF.

3. Cross-Talk Free PS Based on SPHF

The schematic of a cross-talk free directional coupler type PS is shown in Fig. 5. In order to design the PS, three kinds of HFs are required whose core regions are represented by the dashed frames, *i.e.*, a polarization independent HF (PIHF) in the middle which is used as the input waveguide, an xSPHF and a ySPHF at both sides of the PIHF which are used as two output waveguides. The PIHF have an isotropic core with only circular air holes (diameter is represented by d_{PI}), and both x- and y-polarized light can be transmitted. According to the coupled mode theory, when the three waveguides meeting the phase matching condition, an arbitrary polarized incident light can be completely split into the corresponding x- and y-polarized components with an appropriate device length. In the actual fabrication process, unavoidable slight variations occur between the fabricated hole sizes and designed hole sizes, even the phase matching condition cannot be perfectly satisfied, the uncoupled component will remain in the input PIHF, and only the desired polarization component exists for each output waveguide, *i.e.* the cross-talk free property is still achieved.

In order to design the phase matching waveguides, firstly, a reference waveguide should be determined. Here, the xSPHF is chosen as the reference waveguide since its core circular holes should be designed carefully along the x direction. As discussed in the previous section, the core

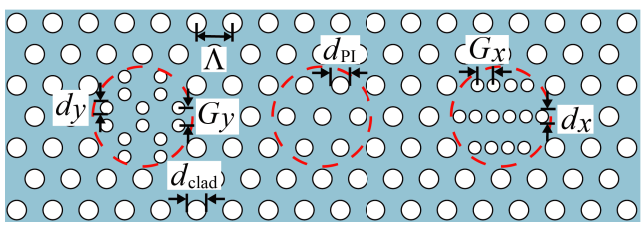

Fig. 5 Schematic of a cross-talk free directional coupler type PS. The core region of each HF is represented by a dashed frame.

hole size and hole gap are set to $d_x = 0.35\Lambda$ and $G_x = 0.5\Lambda$, respectively. In order to achieve the single-polarization operation at the conventional communication band, the FSMs for the core and cladding regions have been investigated. Simulation results show that the single-polarization can be achieved with $d_{\mathrm{clad}} = 0.520 \sim 0.552\Lambda$ at $\lambda = 1.55$ μm. Figure 6 illustrates the dispersion curves of the FSMs of core (dashed curves), and the cladding regions (solid curves) with $d_{\mathrm{clad}} = 0.53\Lambda$, 0.54Λ, and 0.55Λ, respectively. Since the large effective index difference between the FSMs of cladding and the x-polarization of core regions leads to a strong light confinement, therefore, the cladding hole size is set to $d_{\mathrm{clad}} = 0.54\Lambda$.

With the determined structural parameters of the xSPHF, the rings of double-hole unit in the core should be discussed to achieve the SPSM operation. Based on conventional optical fiber theorem, the maximum core radius $R_{\mathrm{core}}^{\mathrm{max}}$ is given as follows,

$$R_{\mathrm{core}}^{\mathrm{max}} = \frac{V_c \lambda}{2\pi n_1 \sqrt{2\Delta}} \tag{2}$$

where Δ is a relative refractive index difference which is given as

$$\Delta = \frac{n_1^2 - n_2^2}{2n_1^2}. \tag{3}$$

Here, n_1 and n_2 represent the effective indices of FSM of core and cladding region, respectively, V_c is the cut-off value, λ is the operating wavelength. For conventional optical fibers, the V-value is required to be smaller than 2.4048 to achieve the single mode operation. Simulation result shows that the SPSM property can be achieved when the number of core ring is less than 3. In this paper, a 1-ring core xSPHF is used to reduce the fabrication difficulty.

Since the three phase matched waveguides in the PS have the same cladding region $d_{\mathrm{clad}} = 0.54\Lambda$, then the single-polarization range of a ySPHF should be investigated

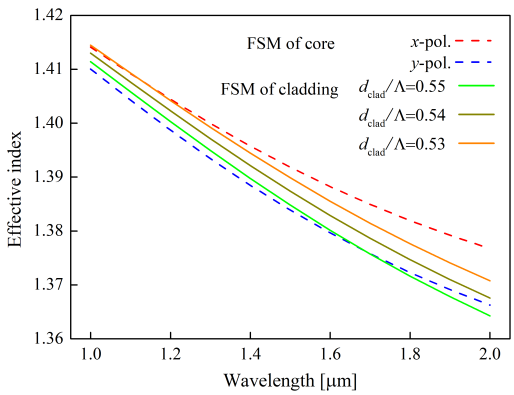

Fig. 6 Effective indices of the core region and cladding region FSM of the xSPHF. The dashed curves are the FSMs of the core (red and blue curves indicate the x- and y-polarization, respectively) and the solid curves are the FSMs with different cladding hole sizes, from the top to bottom, in order, $d_{\mathrm{clad}} = 0.53\Lambda$, 0.54Λ, and 0.55Λ.

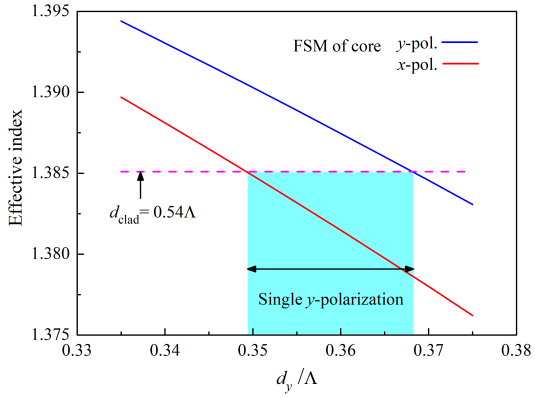

Fig. 7 Effective indices of the core FSM against the hole diameter d_y for the ySPHF with hole gap $G_y = 0.4\Lambda$ at $\lambda = 1.55$ μm.

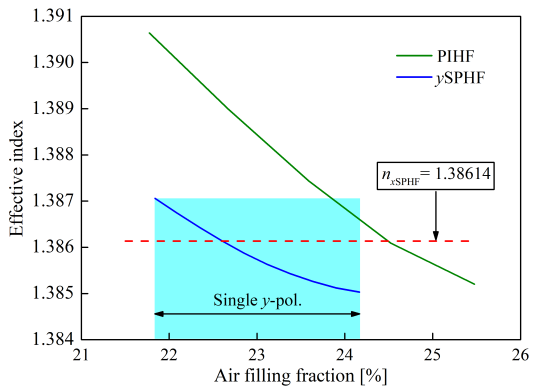

Fig. 8 Effective refractive indices of waveguides for the ySPHF and PIHF as a function of air filling fraction at $\lambda = 1.55$ μm. The single y-polarization operation region is the same as in Fig. 7.

by adjusting the core hole size d_y and hole gap G_y. According to the results in the previous section, a ySPHF has a smaller core birefringence than an xSPHF with the same geometry, therefore, the hole gap G_y is fixed to 0.4Λ to increase its birefringence. Figure 7 shows the variation of the effective indices of core FSM against d_y. The FSM of cladding for $d_{\text{clad}} = 0.54\Lambda$ is represented by the dashed line. We note that single polarization occurs when the FSM of cladding is between the x- and y-polarized core FSMs, and the single y-polarization operation range is illustrated with the blue shaded area. Then, the phase matching core hole sizes of ySPHF and PIHF are determined by setting the waveguide effective indies equal to the xSPHF. The effective refractive indices of waveguides for the ySPHF and PIHF as a function of the air filling fraction are illustrated in Fig. 8. The phase matching core hole size of the ySPHF is $d_y = 0.353\Lambda$ (air filling fraction is 22.6%), and the PIHF is $d_{\text{PI}} = 0.5195\Lambda$ (air filling fraction is 24.5%).

After determined the hole sizes of three waveguides, the core gap between two adjacent cores should also been considered appropriately. A small core gap leads to a high splice loss while a long device length occurs with a large core gap. Here, the core gap is set to 2Λ and the calculated coupling lengths for the x- and y-polarizations are $L_{c,x} = 1758$ μm and $L_{c,y} = 1778$ μm, respectively. We adopt the average of the two coupling lengths as the device length, *i.e.* $L = 1768$ μm. Figure 9 gives the BPM simulation results of the designed PS. The x- and y-polarized components of an incident light are completely separated and coupled into the corresponding SPHFs. With the light propagation, the variation of normalized power for each waveguide is illustrated in Fig. 10. It can be seen that the x- and y-polarized components are completely separated at the propagation distance at 1768 μm. Although there is a coupling length difference between the x- and y-polarizations, the loss is lower than 0.2% for each polarization which is negligible.

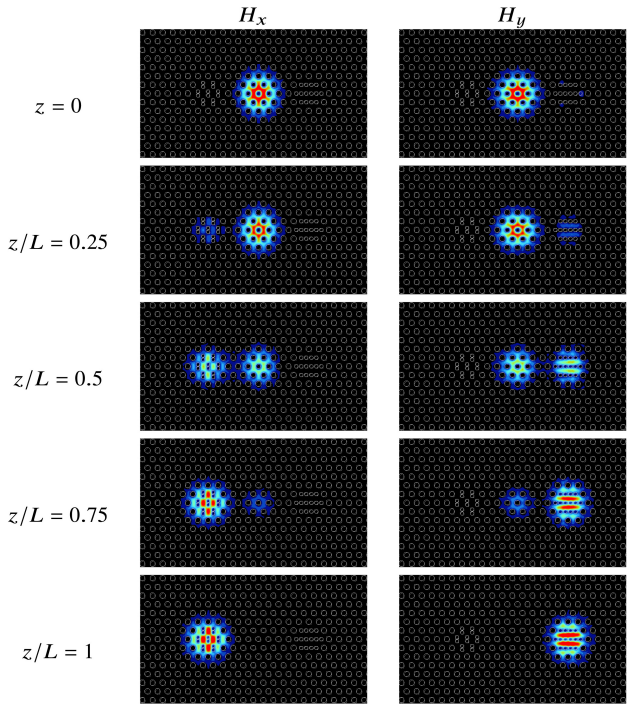

Fig. 9 Propagation behavior in the PS with $\Lambda = 2$ μm ($L = 1768$ μm).

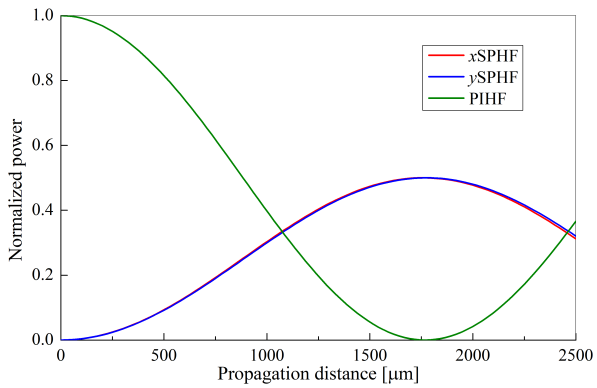

Fig. 10 Normalized power for the input PIHF and two output SPHFs along the propagation distance.

So far, a cross-talk free PS based on double-hole unit core PCFs with $\Lambda = 2$ μm has been designed. Since the variation between actual hole sizes and the corresponding

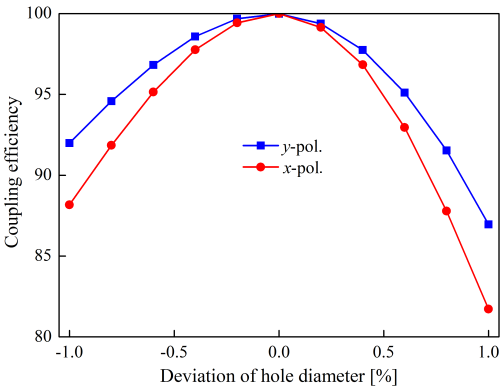

Fig. 11 Coupling efficiency for each polarization versus the deviation of all the air holes at same level.

designed hole sizes is unavoidable during the fabrication process of PCF. It is necessary to discuss the structural tolerances of our designed PS. Additionally, the PS is designed with the wavelength of 1.55 μm, while the coupling efficiency will decrease if the incident wavelength varies, therefore, the wavelength dependence of each polarization is investigated. When the phase matching condition between two adjacent waveguides cannot be perfectly satisfied, then the coupling efficiency F is given as:

$$F = 1 - \left(\frac{n_{\mathrm{eff},1} - n_{\mathrm{eff},2}}{n_{\mathrm{eff,e}} - n_{\mathrm{eff,o}}} \right)^2 \tag{4}$$

where $n_{\mathrm{eff},1}$ and $n_{\mathrm{eff},2}$ illustrate the effective indices of the two waveguides in the isolated system, and $n_{\mathrm{eff,e}}$ and $n_{\mathrm{eff,o}}$ represent the effective indices of the even and odd modes in the coupled system.

In [19], it has been reported that the fabrication accuracy of circular air holes in the PCFs could be controlled within ±1%. Under the same circumstance and considering the various uncertain factors in the fabrication processes, firstly, we estimate the coupling efficiency of PS when all the air holes are deviated within ±1% at the same level. It can be seen in Fig. 11 that the coupling efficiency of x-polarization decreases faster than that of y-polarization with the same hole deviation level. This is because there is a deviation between the effective indices of adjacent two waveguides, especially for the x-polarization. However, all the air hole sizes are varied randomly during the fabrication process; some hole sizes become larger, while some hole sizes turn smaller. Consequently, the random variation of the overall air holes leads to a relatively small effect on the effective index of each waveguide, and the corresponding coupling efficiency will higher than that shown in Fig. 11. According to the coupled mode theory, the coupling efficiency is mainly related to whether the mode matching condition is satisfied or not. Considering that the effective index of a SPHF has a strong core hole size dependence and thus the coupling efficiency of PS against the core hole size variation of each waveguide should be discussed. Table 1 gives the coupling efficiencies of PS versus the deviation for different parts of the device parameters at each deviation level. We note that

Table 1 Coupling efficiency versus the deviation for different parts of the device parameters at each deviation level

Deviation level	Core region			Cladding region
	ySPHF	PIHF	xSPHF	
−0.3%	88.8%	82.7%	87.0%	99.5%
−0.2%	94.6%	92.2%	93.8%	99.7%
−0.1%	98.5%	97.7%	98.3%	99.8%
0	99.9%	99.9%	99.9%	99.9%
0.1%	99.0%	98.0%	98.7%	98.9%
0.2%	95.8%	92.7%	94.8%	98.5%
0.3%	90.9%	87.5%	89.0%	97.7%

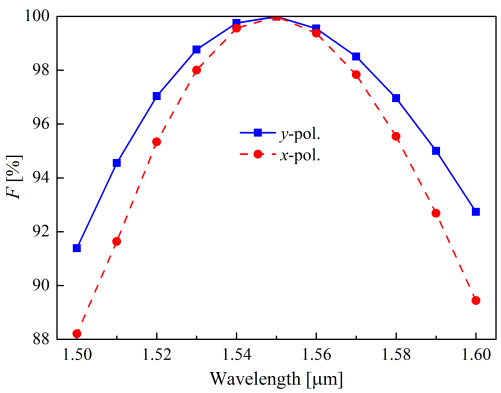

Fig. 12 Coupling efficiency for each polarization as a function of wavelength.

the deviation of core hole size leads to a low coupling efficiency, such as, when the core hole size in ySPHF reduces by 0.3%, then the coupling efficiency decreases to 88.8%. Comparing to the large hole EC-CHF based PS in [14], PS in this study has almost the same coupling efficiency under the same deviation level. However, the use of large lattice pitch of $\Lambda = 2\,\mu$m ($\Lambda = 1.24\,\mu$m in [14]) and PCF with only circular air holes makes it easier to be fabricated.

Additionally, the wavelength dependence of the PS has also been investigated, as shown in Fig. 12. For y-polarization splitting, the coupling efficiency is better than 90% from 1.5 to 1.6 μm, while the coupling efficiency decreased slightly for the x-polarization splitting.

4. Conclusion

In this paper, a novel SPSM HF with only circular air holes has been proposed. By using the double-hole unit to replace the elliptical air holes, a high core birefringence up to the order of 10^{-2} is realized, and the SPHF is also designed with an appropriate cladding hole size. Then, two kinds of 1-ring core SPHFs and a PIHF, which are satisfied the phase matching condition, are designed to consist a cross-talk free PS. Polarization splitting can be completely achieved with a device length of 1768 μm. Moreover, the structural tolerance and wavelength dependence have also been discussed in detail. Even the PS has almost the same tolerance in [14], the structure without elliptical air holes will reduce the fabrication difficulty. So far, tapered PCFs have been proposed and fabricated with a microstructure pitch of less than

300 nm [18]. The structure tolerance of the proposed PS in this paper can be increased if adopting an appropriate taper region into the PS. This is because a strong coupling occurs in the tapered region which has a small lattice pitch. Moreover, PS with a tapered structure can also reduce the overall device length.

References

[1] J.C. Knight, T.A. Birks, P.S.J. Russell, and D.M. Atkin, "Allsilica single-mode optical fiber with photonic crystal cladding," Opt. Lett., vol.21, no.19, pp.1547–1549, Oct. 1996.
[2] P.S.J. Russell, "Photonic-crystal fibers," J. Ligthw. Technol., vol.24, no.12, pp.4729–4749, Dec. 2006.
[3] M. Eguchi and Y. Tsuji, "Single-mode single-polarization holey fiber using anisotropic fundamental space-filling mode," Opt. Lett., vol.32, no.15, pp.2112–2114, Aug. 2007.
[4] M. Eguchi and Y. Tsuji, "Single-polarization elliptical-hole lattice core photonic-bandgap fiber," J. Ligthw. Technol., vol.31, no.1, pp.177–182, Jan. 2013.
[5] S. Kim, C.-S. Kee, and C.G. Lee, "Modified rectangular lattice photonic crystal fibers with high birefringence and negative dispersion," Opt. Exp., vol.17, no.10, pp.7952–7957, May 2009.
[6] D. Chen and G. Wu, "Highly birefringent photonic crystal fiber based on a double-hole unit," App. Opt., vol.49, no.9, pp.1682–1685, March 2010.
[7] Y.S. Lee, C.G. Lee, Y. Jung, and S. Kim, "Diamond unit cell photonic crystal fiber with high birefringence and low confinement loss based on circular air holes," Appl. Opt., vol.54, no.20, pp.6140–6145, July 2015.
[8] K. Saitoh and M. Koshiba, "Single-polarization single-mode photonic crystal fibers," IEEE Photon. Technol. Lett., vol.15, no.10, pp.1384–1386, Oct. 2003.
[9] F. Zhang, M. Zhang, X. Liu, and P. Ye, "Design of wideband single-polarization single-mode photonic crystal fiber," J. Lightw. Technol., vol.25, no.5, pp.1184–1189, May 2007.
[10] M. Eguchi and Y. Tsuji, "Design of single-polarization ellipticalhole core circular-hole holey fibers with zero dispersion at 1.55 μm," J. Opt. Soc. Amer. B, vol.25, no.10, pp.1690–1701, Oct. 2008.
[11] M.-Y. Chen, B. Sun, and Y.-K. Zhang, "Broadband single-polarization operation in square-lattice photonic crystal fibers," J. Lightw. Technol., vol.28, no.10, pp.1443–1446, May 2010.
[12] L. Zhang and C. Yang, "Polarization splitter based on photonic crystal fibers," Opt. Exp., vol.11, no.9, pp.1015–1020, May 2003.
[13] W. Lu, S. Lou, X. Wang, L. Wang, and R. Feng, "Ultrabroadband polarization splitter based on three-core photonic crystal fibers," Appl. Opt., vol.52, no.3, pp.449–455, Jan. 2013.
[14] Z. Zhang, Y. Tsuji, and M. Eguchi, "Study on crosstalk-free polarization splitter with elliptical-hole core circular-hole holey fibers," J. Lightw. Technol., vol.32, no.23, pp.4558–4564, Dec. 2014.
[15] Z. Zhong, Z. Zhang, Y. Tsuji, and M. Eguchi, "Study on crosstalk-free polarization splitter based on square lattice single-polarization photonic crystal fibers," IEEE J. Quantum Electron., vol.52, no.5, 7000107, May 2016.
[16] M. Koshiba and Y. Tsuji, "Curvilinear hybrid edge/nodal elements with triangular shape for guided-wave problems," J. Ligthw. Technol., vol.18, no.5, pp.737–743, May 2000.
[17] Y. Tsuji and M. Koshiba, "Adaptive mesh generation for full-vectorial guided-mode and beam propagation solutions," IEEE J. Sel. Topics Quantum Electron., vol.6, no.1, pp.163–169, Jan. 2000.
[18] E.C. Mägi, P. Steinvurzel, and B.J. Eggleton, "Tapered photonic crystal fibers," Opt. Exp., vol.12, no.5, pp.776–784, March 2004.
[19] S. Lou, Z. Tang, and L. Wang, "Design and optimization of broadband and polarization-insensitive dual-core photonic crystal fiber coupler," Appl. Opt., vol.50, no.14, pp.2016–2023, May 2011.

Zejun Zhang received the B.S. degree from the Department of Electrical Engineering, Xuchang University, Xuchang, China, in 2011, and the M.S. and Ph.D degree from the Division of Information and Electronic Engineering, Muroran Institute of Technology, Muroran, Japan, in 2014 and 2016. Now, He is an Associate Professor of Department of Electrical, Electronics and Information Engineering with Kanagawa University. Dr. Zhang is a member of the Institute of Electrical and Electronics Engineers (IEEE).

Yasuhide Tsuji received the B.S., M.S., and Ph.D. degrees from Hokkaido University, Sapporo, Japan, in 1991, 1993, and 1996, respectively, all in electronics engineering. He joined the Department of Applied Electronic Engineering, Hokkaido Institute of Technology, Sapporo, in 1996. From 1997 to 2004, he was an Associate Professor of Electronics and Information Engineering with Hokkaido University. From 2004 to 2011, he was an Associate Professor of Electrical and Electronic Engineering with the Kitami Institute of Technology, Kitami, Japan. Since 2011, he has been a Professor with the Division of Information and Electronic Engineering, Muroran Institute of Technology, Muroran, Japan. He has been engaged in research on optical wave electronics. Dr. Tsuji is a member of the Institute of Electronics, Information and Communication Engineers (IEICE), the Japan Society of Applied Physics, and the Optical Society of America. In 1997 and 1999, he received the Excellent Paper Award from IEICE. In 2000, he received the Third Millennium Medal from the IEEE.

Masashi Eguchi received the B.S. degree in electronics engineering from the Kitami Institute of Technology, Kitami, in 1985, and the M.S. and Ph.D. degrees in electronics engineering from Hokkaido University, Sapporo, in 1987 and 1991, respectively. He joined Sony Company, Ltd., in 1987. From 1991 to 1995, he was with the Department of Industrial Design, Sapporo School of the Arts, Sapporo. From 1995 to 1998, he was an Associate Professor with the Center for Multimedia Aided Education Educational Center for Information Processing, Muroran Institute of Technology, Muroran, Japan. Since 1998, he has been an Associate Professor with the Faculty of Department of Opto-Electronic System Engineering, Chitose Institute of Science and Technology, Chitose, Japan. He has been engaged in research on various optical fibers, dielectric waveguides, optical solitons, and applications of finite element method and other electromagnetic wave analysis methods. Dr. Eguchi is a Senior Member of the Optical Society of America and a member of the Institute of Electronics, Information and Communication Engineers.

Chun-ping Chen received Ph.D degrees in Microwave and Electro-magnetic Field Engineering from Shanghai University, Shanghai, China, in 2004. Form 2004 to 2006, he was continuing his research as a post-doctor in Kanagawa University, Japan. From 2006, he joined the faculty of Kanagawa University as a research associate. Now, he is an Associate Professor in the same university. His research interests include microwave planar circuit design, materials' EM-property measurement and EMC related techniques. Dr. Chen is a member of IEEE and IEICE. He has served on the Editorial Board of IEEE Transactions on Microwave Theory and Techniques, Review Board of IEEE Microwave and Wireless Components Letters, Review Board of IET Microwaves, Antennas & Propagation and Review Board of IEICE Transactions on Electronics, Associate Editor of IEICE Electronics Express, Japan. He is also serving as a Committee Member of IEEE Microwave Theory and Techniques Society Japan Chapter. He received Young Researcher's Award of IEICE in 2009